Research article

Journal of MASS SPECTROMETRY

Received: 9 January 2017 Revised: 17 February 2017 Accepted: 26 February 2017 Published online in Wiley Online Library

(wileyonlinelibrary.com) DOI 10.1002/jms.3926

# Charge transfer dissociation of phosphocholines: gas-phase ion/ion reactions between helium cations and phospholipid cations

Pengfei Li[a] and Glen P. Jackson[a,b]*

**Phospholipid cations formed by electrospray ionization were subjected to excitation and fragmentation by a beam of 6 keV helium cations in a process termed charge transfer dissociation (CTD). The resulting fragmentation pattern in CTD is different from that of conventional collision-induced dissociation, but analogous to that of metastable atom-activated dissociation and electron-induced dissociation. Like collision-induced dissociation, CTD yields product ions indicative of acyl chain lengths and degrees of unsaturation in the fatty acyl moieties but also provides additional structural diagnostic information, such as double bond position. Although CTD has not been tested on a larger lipid sample pool, the extent of structural information obtained demonstrates that CTD is a useful tool for lipid structure characterization, and a potentially useful tool in future lipidomics workflows. CTD is relatively unique in that it can produce a relatively strong series of 2+ product ions with enhanced abundance at the double bond position. The generally low signal-to-noise ratios and spectral complexity of CTD make it less appealing than OzID or other radical-induced methods for the lipids studies here, but improvements in CTD efficiency could make CTD more appealing in the future. Copyright © 2017 John Wiley & Sons, Ltd.**

**Keywords:** instrumentation development; lipid; novel fragmentation; phosphocholine; radical fragmentation

## Introduction

Lipids are essential components of cellular membranes in living cells.[34,41] In addition to serving as a 'container' for the cell, lipids also show remarkable involvement in a range of lipid–lipid and lipid–protein interactions, thus acting as key players with distinctive biochemical roles and biophysical properties.[6] A detailed description of all lipids and their functions at the cellular level would greatly facilitate the understanding of signaling, lipid metabolism and membrane vesicle trafficking. However, the full structural characterization and quantitation of all lipids in a given system remains a formidable challenge to biochemists.[40]

Mass spectrometry (MS) has emerged as an indispensable analytical tool for the structural characterization of lipids. Soft ionization techniques, such as electrospray ionization (ESI)[40] and matrix-assisted laser desorption/ionization,[3] help ionize lipids in their native states, without requiring derivatization and without causing decomposition, thereby enabling the unequivocal determination of molecular weights. These soft ionization techniques are typically used in conjunction with tandem MS (MS/MS) to provide structural detail and to help resolve isomers. Low-energy collision-induced dissociation (CID) is the most prevalent MS/MS technique, and it has been employed for the structural analysis of a wide variety of lipid classes, including sphingomyelin (SM),[18] phosphatidylglycerol,[20] glycerophosphoethanolamine,[19] glycerophosphocholine[21] and glycerophosphatidic acid.[22]

Low-energy collisional activation of lipids mainly produces fragments corresponding to the loss of entire fatty acyl substituents, like neutral ketenes and fatty acids, and is thus not informative enough for full structure characterization.[16] To enhance the amount of structural information, a variety of MS/MS techniques have been explored as the alternative for the structural interrogation of lipids, including high-energy (HE) CID,[1,2] ion/molecule reactions (e.g. Paternò–Büchi reactions,[30] OzESI/OzID[7,36,39,46–48]), ion/ion reactions,[42,45] ion/photon reactions (e.g. ultraviolet photo -dissociation electron transfer reactions UVPD,[32] IRMPD[51]), electron-based reactions (e.g. electron transfer dissociation (ETD),[29] electron impact excitation of ions from organics (EIEIO),[9] electron-induced dissociation (EID)[24,50]) and radical-directed dissociation.[35,37]

In OzESI/OzID, the exposure of unsaturated lipids to ozone molecules results in an ozonide, which then dissociates into fragment ion pair(s) with diagnostic mass separation that enables an unambiguous identification of sites of unsaturation.[47,48] McLuckey, Blanksby and coworkers have shown that gas-phase ion/ion reactions can be used to convert lipid cations into their anion form, thereby providing incredible selectivity toward certain lipid classes.[42,45] When combined with low-energy CID, ion/ion reactions could provide enhanced structural information, such as acyl chain lengths and degrees of unsaturation.[42,45] Jackson and

* *Correspondence to: Glen P. Jackson, Department of Forensic and Investigative Science, West Virginia University, Morgantown, WV 26506-6121, USA. E-mail: glen.jackson@mail.wvu.edu*

a *C. Eugene Bennett Department of Chemistry, West Virginia University, Morgantown, WV, 26506, USA*

b *Department of Forensic and Investigative Science, West Virginia University, Morgantown, WV, 26506-6121, USA*

coworkers have exploited the use of metastable atom-activated dissociation (MAD) MS[12] and MAD in combination with CID[28] for the analysis of phospholipids. The HE radical-induced dissociation technique produced a range of fragments that are closely related to the number and location of double bonds in lipid acyl chains. Whereas the current state of the art in tandem MS has a variety of approaches to target certain functional groups and chemistries, the communities interested in lipid characterization and lipidomics would stand to benefit from additional or complementary approaches to tandem MS.

Charge transfer dissociation (CTD) is a possible alternative to the aforementioned MS/MS techniques, and it proceeds via exposure of gas-phase precursor cations to a kiloelectronvolt beam of helium cations.[17] Upon the interaction with helium cations, peptide cations decompose via radical-driven pathways that are significantly different from low energy CID, but analogous to other HE fragmentation methods.[17] CTD has also been demonstrated for complex oligosaccharides.[43] CTD has the ability to increase the number of positive charges on a precursor ion and is workable with singly charged precursor ions, unlike ETD and ECD. The activation energy in CTD is determined by both the electron affinity of the helium cation (~24.6 eV) and kinetic energy and can drive reactions with appearance potentials greater than 24 eV.[17,43]

In this study, we demonstrate the utility of CTD as a means of structural characterization for phosphatidylcholines. Helium cation irradiation of protonated lipids produces highly extensive cleavage along lipid acyl chains (i.e. POPC, PSPC) and charge-increased ion series for lipids containing multiply carbon–carbon (CC) double bonds (i.e. 9E- and 9Z-DOPC). The 12 Da peak spacing feature and the change in fragment ion intensity in the vicinity of the CC double bond appear to be closely related to the position and geometry of CC double bond(s), but with some questions remaining as to the exact mechanism of cleavage at the double bond position.

## Experimental

### Instrumentation

All mass spectra (CID, CTD and MAD) were collected on a Bruker amaZon ETD mass spectrometer (BrukerDaltronics, Bremen, Germany), which has been modified to perform lipid cation/helium cation or lipid cation/metastable atom reactions. Installation of saddle field fast ion/fast atom source (VSW/Atomtech, Macclesfield, UK) connection between electronic components and the working principle is highly analogous to our recent work on peptides and oligosaccharides.[27,43]

### Materials

All the lipids used in this experiment were purchased from Avanti Polar Lipids (Alabaster, AL). The involved lipids and their shorthand designations are as follows: 1-hexadecanoyl-2-octadecanoyl-sn-glycero-3-phosphocholine (PSPC, 160/180), 1-hexadecanoyl-2-(9Z-octadecenoyl)-sn-glycero-3-phosphocholine (POPC, 160/181(9Z)), 1,2-di-(9E-octadecenoyl)-sn-glycero-3-phosphocholine (9E-DOPC, 181/181(9E,9E)), 1,2-di-(9Z-octadecenoyl)-sn-glycero-3-phosphocholine (9Z-DOPC, 181/181(9Z, 9Z)), 1,2-di-(5Z,8Z, 11Z,14Z-eicosatetraenoyl)-sn-glycero-3-phosphocholine (DAPC, 204/204) and N-stearoyl-D-erythro-sphingosylphosphorylcholine (SM, d18:1/18:0). Lipid analytes were prepared at a concentration of ~60 μM in a solution of 49.5/49.5/1 (*v*/v/v) methanol/water/acetic acid prior to positive ESI.

## Method

Each lipid solution was continuously infused into the ESI source with an electronic syringe pump (#1725, Hamilton Company Reno, Nevada, NV) at a flow rate of 160 μL/h. The skimmer was at ground potential, and the electrospray needle was set at 4.5 kV. The temperature of the heated capillary was 220°C. The $[M + H]^+$ or $[M + Na]^+$ ions were mass-selected using an isolation window of 1.0 or 4.0 Da depending on the need for isotope information. The saddle field ion source was only switched on during an $MS^2$ scan function in which the isolated ions were stored at a desired low mass cut-off (e.g. 150) with the excitation amplitude for CID set to zero volts. A 6 kV square wave with a pulse width of 25 ms was applied to the saddle field ion source for the generation of reagent helium cations. The helium flow was controlled via a variable leak valve, and the pressure read-out was obtained from pressure monitor of the ion trap gauge in the main vacuum region. Using this indirect measurement, the helium gas supply was adjusted to provide a reading of $\sim 1.20 \times 10^{-5}$ mbar for all the experiments, which was barely above the base pressure of $\sim 8 \times 10^{-6}$ mbar in the main vacuum chamber. A typical low mass cut-off value of *m/z* 150 was used for the removal of ionized residual background compounds. All the mass spectra (CID, CTD and MAD) were accumulated in profile mode with up to 4 min of averaging to improve the signal-to-noise ratio.

## Results and discussion

Helium cation irradiation of protonated POPC results in a range of fragments, as shown in Fig. 1(a). The CTD spectrum looks generally similar to the MAD spectrum (Fig. 1(b)), but both differ greatly from traditional CID (Fig. 1(c))[16] or electron ionization (EI) spectra.[25,26] All fragmentation methods give a dominant fragment ion at *m/z* 184.0, which is a diagnostic fragment of the phosphocoline head group.[10,12] The CTD spectrum also shows a doubly charged fragment at *m/z* 380.4, which corresponds to the charge-increased product $[POPC + H]^{2+\bullet}$, which is similar to the Penning ionized product ion observed in MAD.[12] CTD shows three major fragments at *m/z* 478.4, *m/z* 496.4 and *m/z* 521.4, which are associated with entire acyl chain losses. These fragments resemble closely the MAD fragmentation pattern, but greatly differ from that of CID. Helium-CTD also shows an extensive dissociation along two acyl chains ranging from *m/z* 550 to *m/z* 732, which is also similar to MAD.

Helium-CTD of sodiated POPC produces a fragmentation pattern that highly resembles that of MAD spectrum of $[POPC + Na]^+$, as shown in Fig. S1. In addition to the phosphocoline head group fragment at *m/z* 184.0 and the ionized species $[M + Na]^{2+\bullet}$ at *m/z* 391.5, CTD produced a variety of fragments related to cleavages of the glycerol backbone and its vicinity. Examples include the loss of trimethylamine ($N(CH_3)_3$) at *m/z* 723.5, the entire head group at *m/z* 599.5, sn-1/sn-2 acyl chains at *m/z* 526.5 and *m/z* 500.5 and simultaneous loss of two units, such as at *m/z* 441.4 and *m/z* 467.5. The cleavage of the C1–C2 bond within the glycerol backbone at *m/z* 513.5 was observed in the CTD and MAD spectra, but not in CID. The CTD spectra of protonated POPC and sodiated POPC show different product ion distributions, as has been observed in low-energy CID[16,18,21] and post source decay experiments.[3] The distinction in post source decay spectra for the two adduct forms is attributed to the different binding of $H^+$ and $Na^+$ to lipid head group.[3]

Journal of MASS SPECTROMETRY

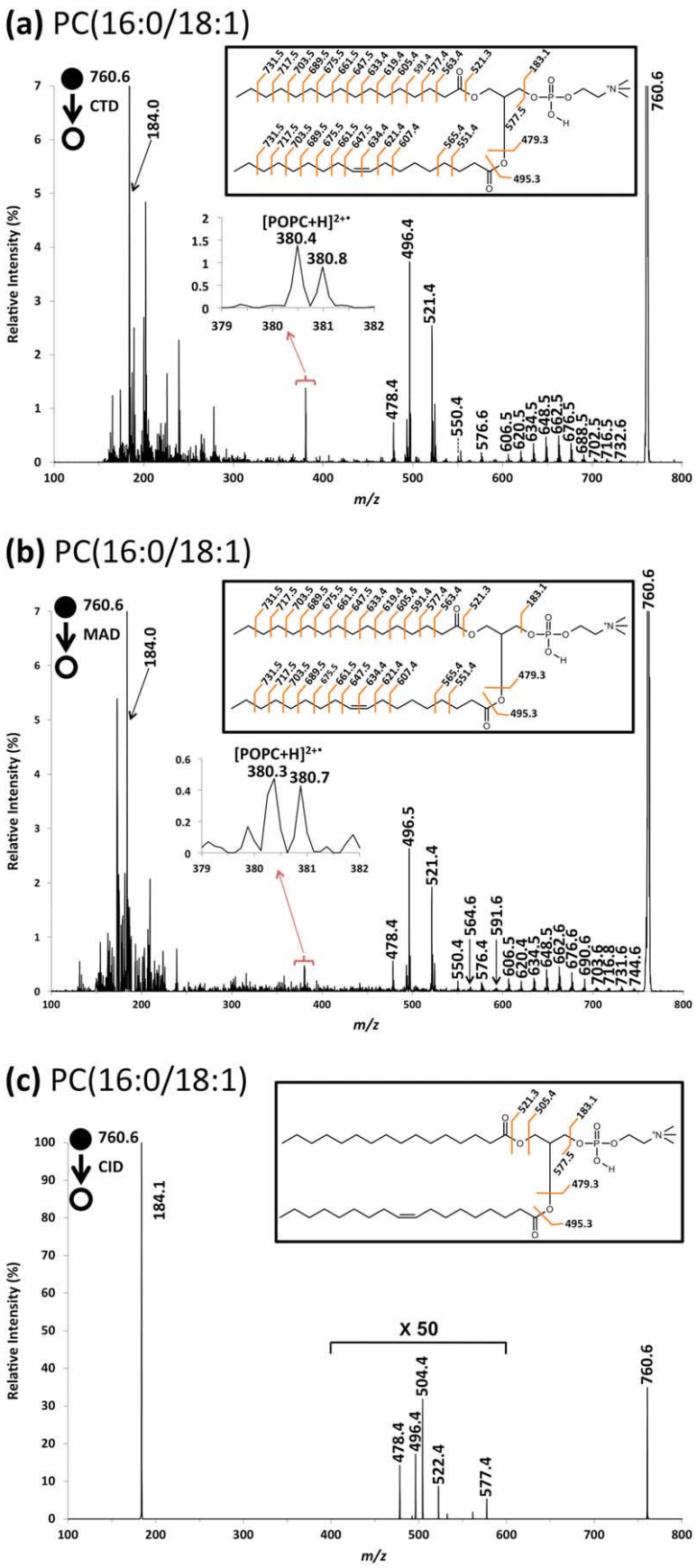


**Figure 1.** (a) Charge transfer dissociation (CTD) spectrum of $[POPC + H]^+$ (160/181). (b) Metastable atom-activated dissociation (MAD) spectrum of $[POPC + H]^+$ (160/181). (c) Collision-induced dissociation (CID) spectrum of $[POPC + H]^+$ (160/181). The diagram insets show possible cleavages and theoretical masses for fragmentations without hydrogen rearrangements. [Colour figure can be viewed at wileyonlinelibrary.com]



  

The results in Figs 1 and S1 indicate that the CTD process involves both CID-like even-electron fragmentation pathways and MAD-like radical-induced fragmentation pathways.[12] Ionization of 1+ precursor ions by Penning ionization or charge transfer is expected to be different in energy by the ionization potential of a helium metastable atom, which is about 4.77 eV.[44] Although this difference seems significant, He metastable atoms and He cations are both more than 19.8 eV above the ground state, so both have more than enough energy to ionize most 1+ precursor ions, which typically have ionization energies of around 10 eV. [8]

A more detailed comparison between CTD and MAD spectra of $[POPC + H]^+$ is given using the zoomed-ins in Figs 2(a–b) and 3 (a–b). In the region from *m/z* 470–540 (Fig. 2(a–b)), the CTD spectrum of $[POPC + H]^+$ shows strong similarity to the MAD spectrum of the same lipid. The common features include neutral ketene losses at *m/z* 522 (sn-1) and *m/z* 496 (sn-2), as well as elimination of sn-2 fatty acid at *m/z* 478.[12] Because the same batch of purchased POPC sample was used for both MAD and CTD experiments, the same set of contamination peaks at *m/z* 493.4 (loss of C(180) chain) and *m/z* 524.4 (loss of C(161) chain) was observed,[12] possibly originating from the isomerization of POPC during its synthesis process.[9,31,38] The spectrum in Fig. 2(d) is a replicate experiment of Fig. 2(c), but with a much narrower isolation window (width = 1.0 Da). The exclusion of the $^{13}C$ contribution in Fig. 2(d) helps confirm the peak assignments in Fig. 2(c).

Different from the CID spectrum of PSPC (Fig. S4(b)), the CTD spectrum in Fig. 2(c) shows two sets of fragments associated with sn-1/sn-2 ketene losses: odd-electron fragments at *m/z* 495.5 and *m/z* 523.5, and even-electron fragments at *m/z* 496.5 and *m/z* 524.5. For both POPC and PSPC, the CTD spectra show preferential neutral ketene loss over neutral fatty acid loss, which resembles radical-induced EID[24] but significantly differs from even-electron CID (Fig. S4). Compared with the CTD spectra of PSPC and POPC in Fig. 2, the same even-electron fragments in the CID spectrum in Fig. S4 are considerably less abundant. Hsu and Turk have shown that these same even-electron ions can be enhanced in CID through lithiation of the lipids.[22] The CID efficiency of lithiated precursors was sufficient to enable additional stages of CID to yield additional structural information.[22]

For the even-electron fragments in Fig. 2(c), CTD does not show a distinctive preference in the formation of *m/z* 496 (sn-2 ketene loss) or *m/z* 522/524 (sn-1 ketene loss), which compromises its ability to differentiate between the sn-1 and sn-2 ketene losses. In this regard, CTD is slightly less informative

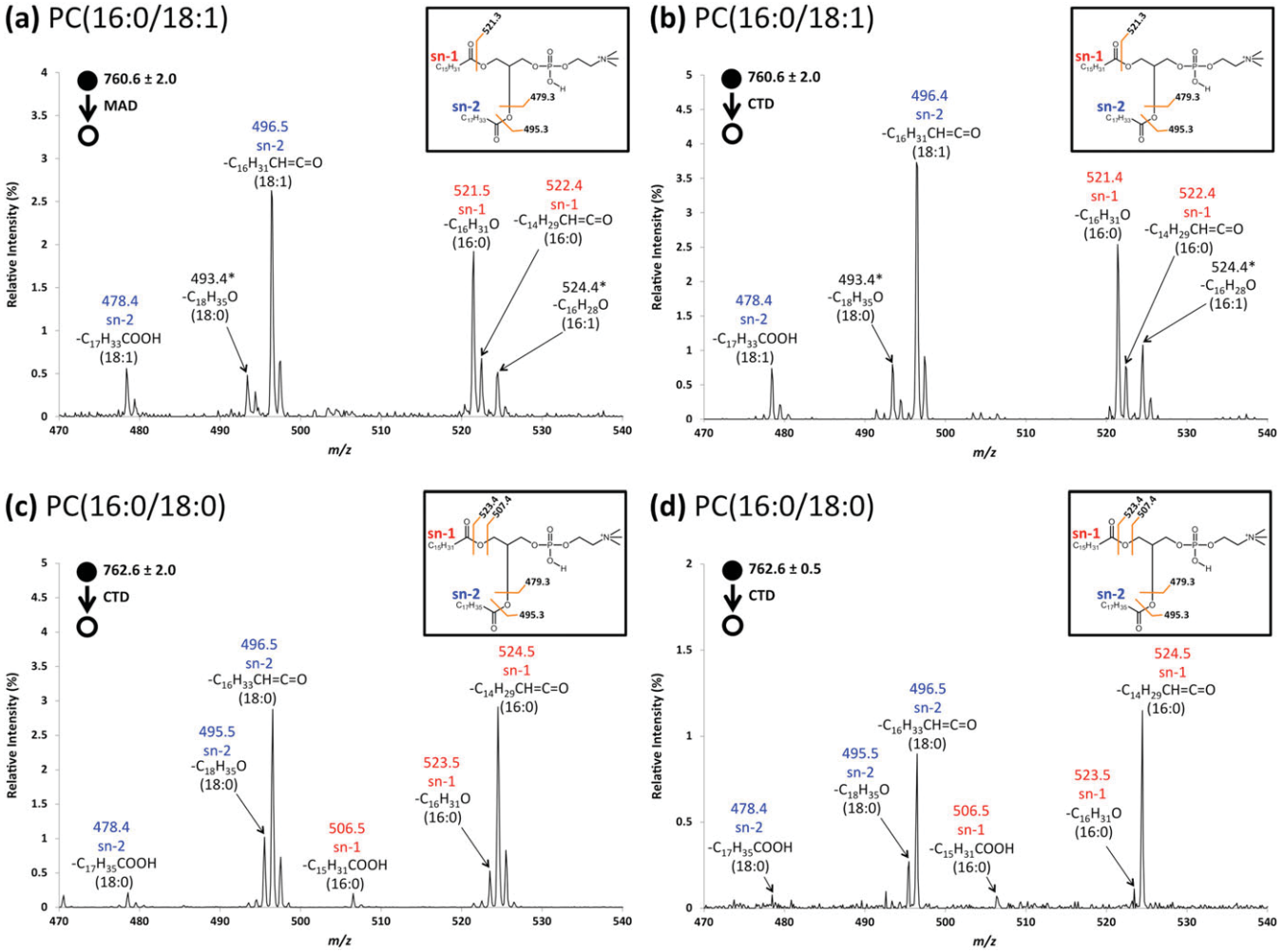


**Figure 2.** Zoomed-in regions from *m/z* 470–540: (a) Metastable atom-activated dissociation (MAD) spectrum of $[POPC + H]^+$ (160/181); (b) Charge transfer dissociation (CTD) spectrum of $[POPC + H]^+$ (160/181); (c) CTD spectrum of $[PSPC + H]^+$ (160/180) with a precursor isolation window width = 4.0; (d) CTD spectrum of $[PSPC + H]^+$ (160/180) with a precursor isolation window width = 1.0. [Colour figure can be viewed at wileyonlinelibrary.com]

Journal of MASS SPECTROMETRY

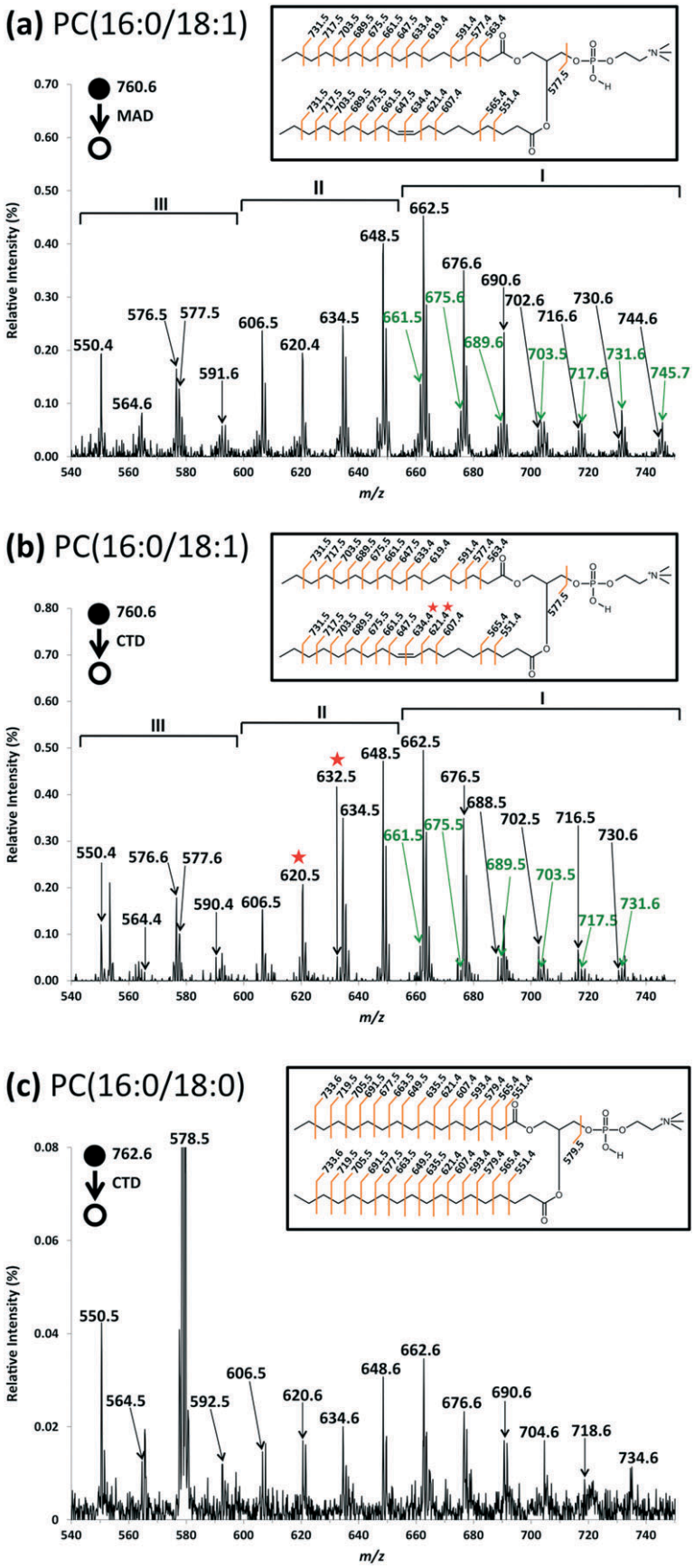


**Figure 3.** Zoomed-in regions from *m/z* 540–750: (a) Metastable atom-activated dissociation (MAD) spectrum of $[POPC + H]^+$ (160/181); Charge transfer dissociation (CTD) spectra of (b) $[POPC + H]^+$ (160/181) and (c) $[PSPC + H]^+$ (160/180). The green font shows radical losses of the type $[C_nH_{2n+2}]$. The red stars correspond to 12 Da peak spacing for locating the C = C double bond(s). [Colour figure can be viewed at wileyonlinelibrary.com]

than CID, which preferentially produces sn-2 ketene loss over sn-1 ketene loss (*m/z* 496 > *m/z* 522 or 524) (Fig. S4).[10,21,24] In contrast to this general preference for sn-2 ketene loss over sn-1 ketene loss, Ho and Huang show no such preference for sn-2 ketene loss in low-energy CID experiments in a quadrupole ion trap[16] and Jones *et al.* observed a slight preference for sn-1 ketene loss over sn-2 ketene loss in the EID fragmentation of phospholipids.[24]

The odd-electron fragments in Fig. 2(c) were also observed in MAD[12] and EID[24] spectra of the same lipid, which suggests analogous fragmentation pathways among CTD, MAD and EID. The odd-electron fragments must be generated via the introduction of radical species during the fragmentation process, indicating the involvement of radical cleavages in CTD.[12] Interestingly, the fragment at *m/z* 495.5 (sn-2 position) is more abundant than the one at *m/z* 523.5 (sn-1 position). This trend agrees with that from the said EID results: the more favorable formation of radical cation associated with sn-2 position.[24] This coincidence, along with the more favorable neutral ketene loss over fatty acid loss in CTD, is indicative of high resemblance of CTD in its mechanistic nature to that of EID.

For ease of discussion, the two spectra in Fig. 3(a–b) are labeled in three sections: I, II and III. The section labeled I shows the acyl cleavages close to the ω-end of the lipid chains. The CTD spectrum of $[POPC + H]^+$ (Fig. 3(b)) shows extensive fragmentation along the two acyl chains in this region, including the even-electron rearrangement fragments at *m/z* 730.5, *m/z* 716.5, *m/z* 702.5, *m/z* 688.5, *m/z* 676.5 and *m/z* 662.5, which correspond to the neutral loss of $C_nH_{2n+2}$ molecules. In the same region, odd-electron fragments at *m/z* 731.5, *m/z* 717.5, *m/z* 703.5, *m/z* 689.5, *m/z* 675.5 and *m/z* 661.5 are also observed (green font), which is corresponding to neutral loss of $C_nH^{\bullet}_{2n+1}$ alkyl radicals. Almost the same even-/odd-electron fragment series were observed in both MAD (Fig. 3(a)) and EID spectra reported elsewhere.[24]

The ladder-like patterns of even-electron fragments are separated by 14.0 Da, which is a commonly observed pattern in EI[25,26] and HE-CID,[49] as well as the recently reported electron-based MS/MS experiments on lipids, EIEIO[9] and EID.[24] The accompanying odd-electron fragments associated with the losses of alkyl radicals were also reported in other HE MS/MS experiments.[9,24,49] Others have proposed that the serial neutral loss of $C_nH_{2n+2}$ could either be the neutral loss of an alkane or be the neutral loss of an alkene + $H_2$ (i.e. 1,4-cyclic elimination).[23,24] In most general respects, CTD fragmentation can therefore be rationalized through radical mechanisms proposed by others.[11,49]

In Section II, the vinyl bond vicinity, CTD-generated fragments exhibit identical nominal masses to that of MAD, but some notable differences were also observed between MAD and CTD. For example, MAD shows reduced intensities at the CC double bond site along with the elevated ion intensity corresponding to distal allyl cleavages—the most prevalent dissociation pattern of unsaturated acyl chains, which has been widely reported in FAB,[33] HE-CID,[11] EIEIO[9] and EID[24] experiments. In CTD, this vicinity looks slightly different and contains a distinctive pair of peaks at *m/z* 620.5 and *m/z* 632.5, whose spacing is a diagnostic 12 Da. This characteristic peak spacing has been well studied and documented as the diagnostic value for localization of CC double bonds. Mass spectrometric experiments involving EI,[13] HE-CID,[14] radical-directed dissociation[35,37] and MAD-$MS^3$ CID[28] have made use of this diagnostic feature for the determination of double bond positioning in unsaturated fatty acid derivatives and phospholipids. Aside from the previous radical-directed fragmentation techniques, the localization of double bond(s) in lipid acyl chains has also been made possible using low-energy CID experiments,[22] although the methodology is completely different from that in the aforesaid techniques. Monolithiated and dilithiated glycerophospholipids were subjected to multiple-stage collisional activation ($MS^n$, $n$ = 3,4), which offered information for pinpointing double-bond location along fatty acyl substituents.

Similar to MAD, CTD only produces a few fragments in Section III, the α-end of the acyl chain, including contributions from both sn-1 and sn-2 acyl chain cleavages. It is generally rare to observe dissociation in this region of the lipid, but the fragments observed for CTD are analogous to the recently reported EID results of $[POPC + H]^+$.[24] The fragments at *m/z* 577.6 and *m/z* 576.5 presumably result from cleavage related to head group loss.

Consistent with CTD results of POPC, CTD of PSPC (Fig. 3(c)) also produces extensive dissociation along two acyl chains, with an even greater extent of fragmentation. PSPC is structurally different from POPC in that it contains two fully saturated acyl chains (16 : 0/18 : 0). Consequently, a more extensive ladder-like dissociation pattern can be seen from *m/z* 718.6 to *m/z* 550.5, which corresponds to the mutual contribution of sn-1 and sn-2 acyl chains. Moreover, the fragment ion intensities appear to be more uniform along the entire saturated acyl chains.[9] It is worth noting that the nominal masses from *m/z* 592.5 to *m/z* 718.6 are in one-to-one correspondence with those in EID of PSPC.[24] A difference between POPC and PSPC is that CTD of PSPC does not produce the aforementioned odd-electron fragment series. The lack of odd-electron fragments in PSPC is analogous to EID experiments.[24] For PSPC, the loss of the head group at *m/z* 578.5 appears more abundant than for POPC, but the difference in abundance relative to the acyl cleavages is due to a decrease in the abundance of acyl fragments for PSPC, not an increase in the abundance of the head group loss.[24]

CID and CTD spectra of protonated 9E-DOPC (181/181) are shown in Fig. 4(a–b). Collisional activation of this lipid only produces three fragments, as we reported before.[12] However, CTD of the same lipid produces a much more extensive fragmentation coverage than CID, which includes head group losses at *m/z* 184.0, *m/z* 521 for the sn-1/sn-2 alkyl ketene loss and *m/z* 505 for the sn-1/sn-2 fatty acid loss. CTD also produces charge-increased, or oxidized, product ions such as $[9E\text{-}DOPC + H]^{2+\bullet}$ at *m/z* 393.5, $[9E\text{-}DOPC + H\text{-}C_9H_{19}]^{2+\bullet}$ at *m/z* 330.5, and acyl chain cleavages at the C = C double bond position. This pattern is almost identical to a previously reported MAD spectrum of $[9E\text{-}DOPC + H]^+$ (11/18:1).[12] The close similarity between MAD and CTD suggests a similar mechanistic nature between them, although the mechanism of cleavage at the double bond position has not yet been elucidated.

The middle panels (c and d) of Fig. 4 compare the range *m/z* 500–530 for CID and CTD results of 9E-DOPC. The bottom panels of Fig. 4 (e–f) show CID and CTD spectra of 9Z-DOPC. In CTD, the peak patterns around *m/z* 521 and *m/z* 505 resemble MAD spectra of the same species[12] but vastly differ from that of CID. CID mainly proceeds through even-electron rearrangements, thus yielding even-electron fragments. The zoomed-in CTD spectrum of cis-double bond lipid (9Z-DOPC) looks very similar to that of trans-double bond lipid (9E-DOPC), which agrees with the reported difficulty in differentiating cis- and trans-geometry of double bonds.[15] For CTD of both 9E- and 9Z-DOPC, the preference in ketene loss (*m/z* 522.5) over fatty acid loss (*m/z* 506.5) is in contrast to CID spectra. This preferential ketene loss in CTD is consistent with the aforesaid trend for POPC and PSPC. The reproducible feature across lipids with different acyl chain combinations further confirms

Journal of MASS SPECTROMETRY

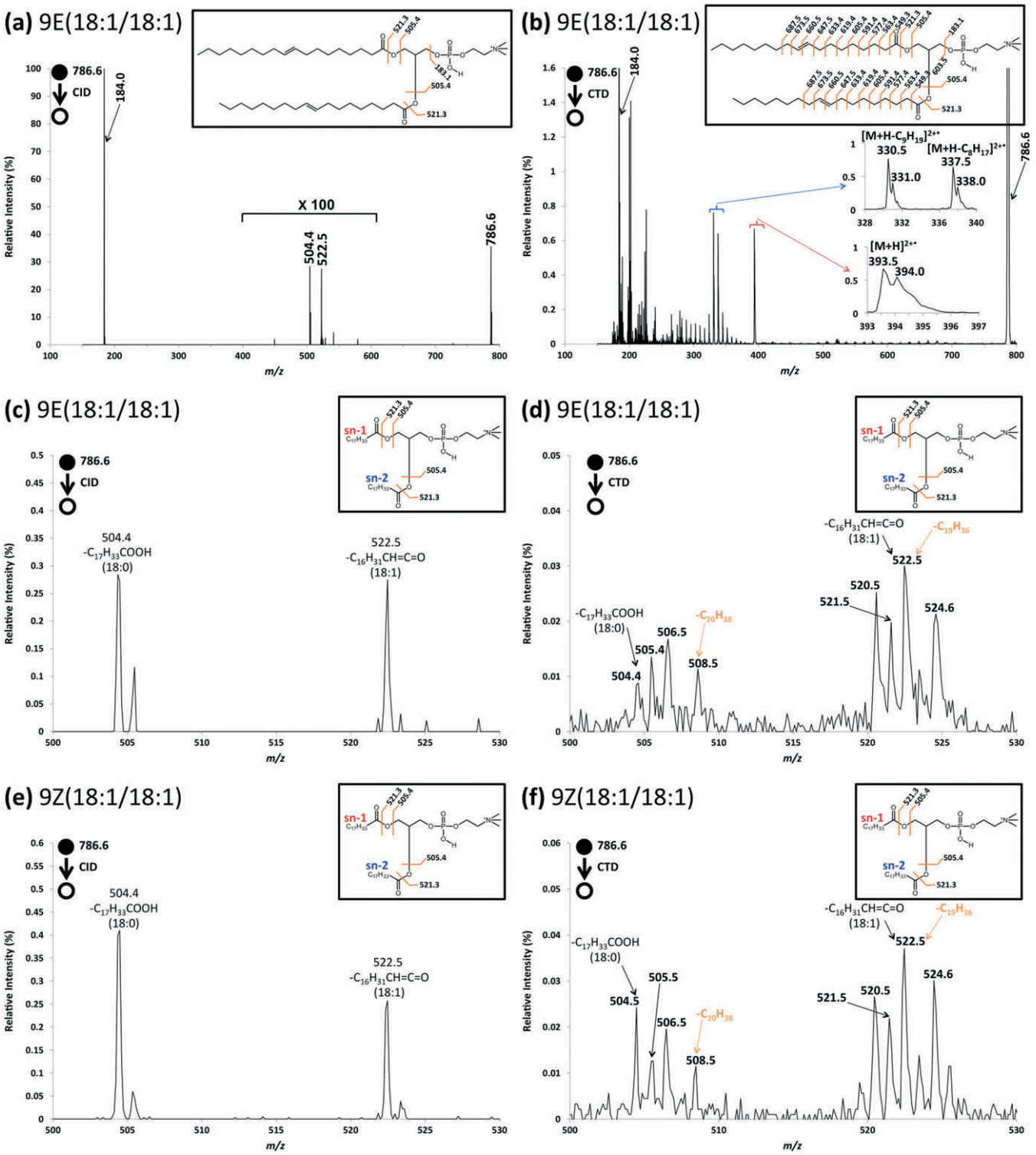


**Figure 4.** (a) Collision-induced dissociation (CID) spectrum of $[9E\text{–}DOPC + H]^+$ + (181/181). (b) Charge transfer dissociation (CTD) spectrum of $[9E\text{–}DOPC + H]^+$ + (181/181). Zoomed-in regions from *m/z* 500–530: (c) CID spectrum of [9E–DOPC + H] + (18 : 1/18 : 1); (d) CTD spectrum of [9E–DOPC + H] + (181/18 : 1); (e) CID spectrum of $[9Z\text{–}DOPC + H]^+$ + (181/181); (f) CTD spectrum of $[9Z\text{–}DOPC + H]^+$ (181/181). The orange font in panels (d) and (f) shows the $C_nH_{2n-2}$-type losses and their tentative assignments. [Colour figure can be viewed at wileyonlinelibrary.com]

the distinctive mechanistic nature of CTD, which should be different from that of even-electron CID, but is close to radical dissociation feature of MAD, EIEIO and EID.

Figure 5(a–b) shows magnified CTD spectra of $[9E\text{-}DOPC + H]^+$ and $[9Z\text{-}DOPC + H]^+$ from *m/z* 530 to 750. In contrast to PSPC, which has two saturated acyl chains, 9E- and 9Z-DOPC both contain two unsaturated acyl chains. Consistent with CTD results of POPC and PSPC, a ladder-like fragmentation pattern was observed in CTD spectra of both 9E- and 9Z-DOPC. Different from the CTD results of POPC and PSPC, fewer fragments were observed for 9E- and



  

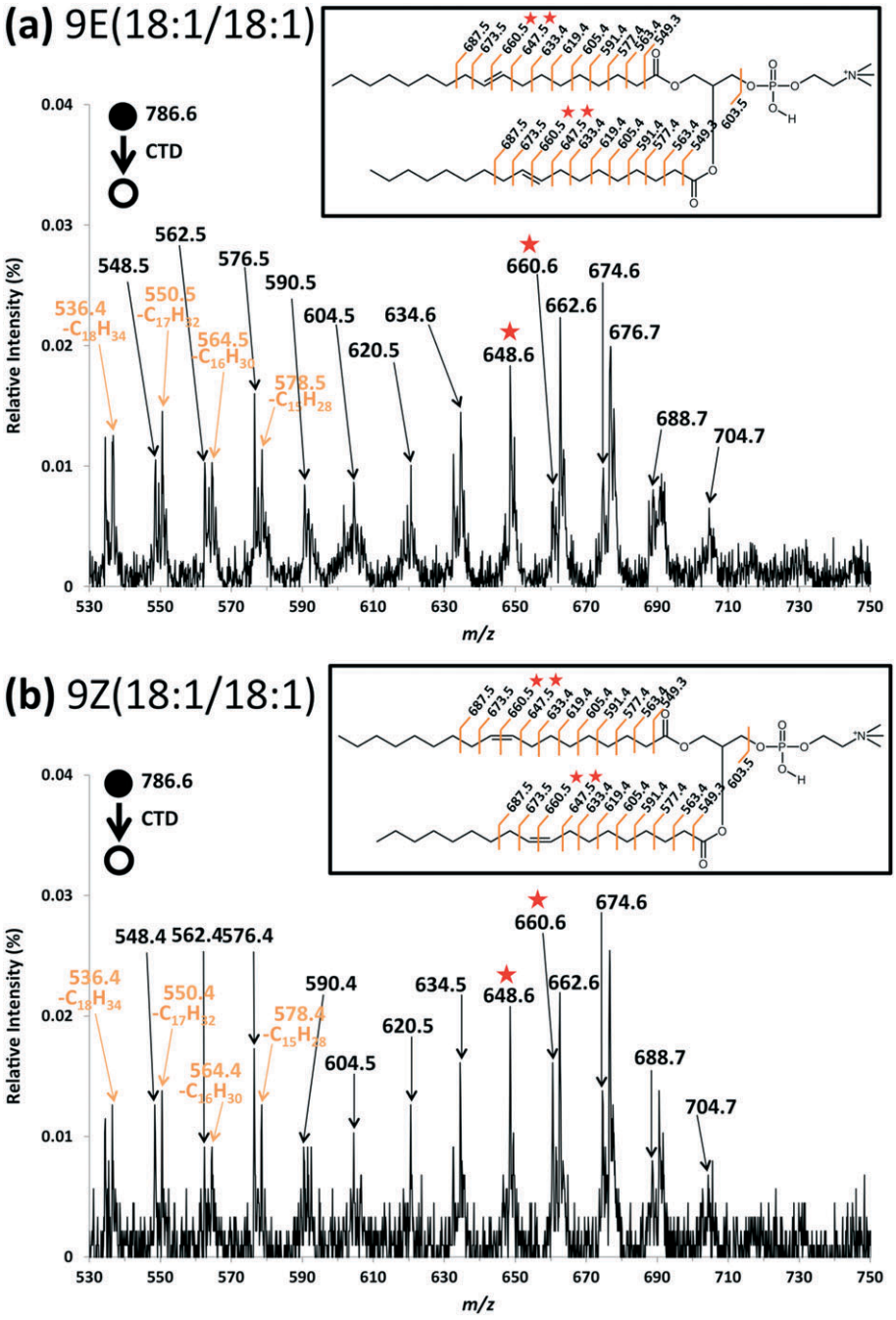


**Figure 5.** Zoomed-in regions from *m/z* 530–750 of charge transfer dissociation (CTD) spectra of (a) $[9E–DOPC + H]^+$ (181/181); (b) $[9Z-DOPC+ H]^+$ (181/181). The orange font shows the $C_nH_{2n-2}$-type losses and their tentative assignments. [Colour figure can be viewed at wileyonlinelibrary.com]

9Z-DOPC. The lack of CC single bond cleavages closer to ω-end was also seen in EID spectra of 9Z- and 6Z-DOPC.[24] It seems that the presence of multiple CC double bonds obstructs the propensity of fragmentation in CTD and other radical-induced approaches.

Consistent with the CTD results of POPC, the diagnostic peak spacing of 12 Da was also observed in the double bond region for both 9E- and 9Z-DOPC, which offers an unambiguous localization of CC double bonds in both lipids. The consistency in this 12 Da spacing demonstrates the reproducibility of CTD in producing this double bond-specific feature. These results also indicate the promising potential of CTD for the diagnosis or differentiation of sites of unsaturation in lipids or further possible extension into other biomolecules with unsaturated olefinic chains, such as fatty acids methyl esters.

In contrast to the CTD spectra of POPC and PSPC, CTD spectra of 9E- and 9Z-DOPC show a unique neutral losses, including: *m/z* 508 ($-C_{20}H_{38}$), *m/z* 522 ($-C_{19}H_{36}$), *m/z* 536 ($-C_{18}H_{34}$), *m/z* 550 ($-C_{17}H_{32}$), *m/z* 564 ($-C_{16}H_{30}$) and *m/z* 578 ($-C_{15}H_{28}$) (orange font in Figs 4(c–d) and 5(a–b)). The tentative assignments are shown in parentheses, earlier. This type of $C_nH_{2n-2}$ neutral loss is consistent with the observation in EID experiments, which could be attributed to the mutual cleavages of both unsaturated acyl chains.[24]

Figure 6 compares the unique doubly charged ion series in CTD of $[9E-DOPC + H]^+$ and $[9Z-DOPC + H]^+$, which shows a peak

Journal of MASS SPECTROMETRY

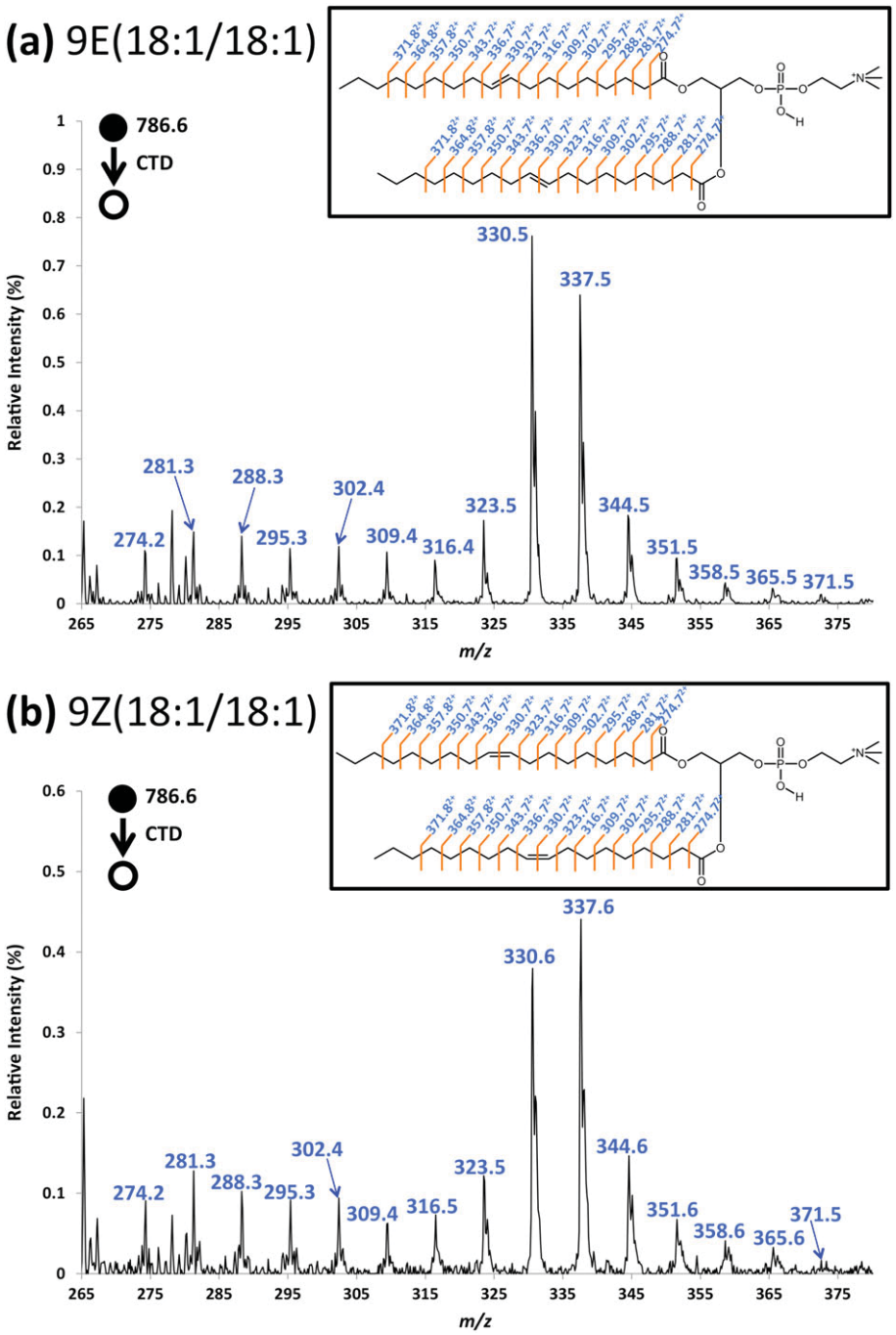


**Figure 6.** Zoomed-in regions from *m/z* 265–380 of charge transfer dissociation (CTD) spectra of the following: (a) $[9E–DOPC + H]^+$ (181/181); (b) $[9Z-DOPC + H]^+$ (181/181). [Colour figure can be viewed at wileyonlinelibrary.com]

spacing of 7.0 Da instead of 14.0 Da. To our best knowledge, doubly charged product ions showing a 7.0 Da-ladder pattern is rarely reported in gas-phase ion activation experiments. Nevertheless, this pattern was also observed in MAD spectra of 9E- and 9Z-DOPC,[12] again suggesting a significant mechanistic similarity between CTD and MAD. The doubly charged ion series almost covers the entire acyl chain. 9E- and 9Z-DOPC spectra exhibit a similar extent of chain cleavage and also show a similar fragment ion intensity distribution. Noticeably, the most abundant peaks are at *m/z* 330 and *m/z* 337, corresponding to cleavages at or next to the site of unsaturation in both lipids.

In the spectrum for 9E-DOPC (Fig. 6(a)), the peak at *m/z* 330 is more abundant than *m/z* 337; while in 9Z-DOPC spectrum, the trend appears to be reversed. The variation in fragment ion intensities was reproducible on different days and is therefore more likely to be sensitive to the geometry of double bond rather than experimental irreproducibility. Because 9E- and 9Z-DOPC only differ in double bond geometry, identical fragment masses are generated for both lipids. Given the similar dissociation pattern and lack of diagnostic fragments, the most common way to discriminate them is to track the changes in relative abundances of certain fragments. This concept has been reported



  

and utilized in the differentiation of geometrical isomers of fatty acids methyl esters using low-energy EI MS.[15]

Figure 7 shows the comparison between CTD and CID spectra of protonated sphingomyelin (SM). Collisional activation of SM produces very few fragments: *m/z* 184.0, associated with phosphocholine head group loss, and *m/z* 713.6, associated with a neutral water loss.[12] The inefficiency of CID in producing structurally informative fragments is consistent with literature reports.[4,18,33]

However, CTD of the same precursor of SM is capable of producing a few additional fragments, including a characteristic charge-increased product ion ($[M + H]^{2+\bullet}$) at *m/z* 365.9 and two fragments at *m/z* 447.4 and *m/z* 491.4, corresponding to the entire acyl chain losses. These distinctive product ions are only observed in CTD and not observed in MAD of the same species.[12] SM is structurally different from the other tested phospholipids: one fatty acyl group is alkylated to the lipid backbone, with the other fatty acyl group being connected to sphingosine via an amide bond.[33] The absence of the two ester connections could possibly make a less 'fragile' molecule, resulting in a less efficient dissociation pattern of CID,[18] MAD and CTD experiments. However, exceptions do exist. Baba and coworkers reported a highly efficient

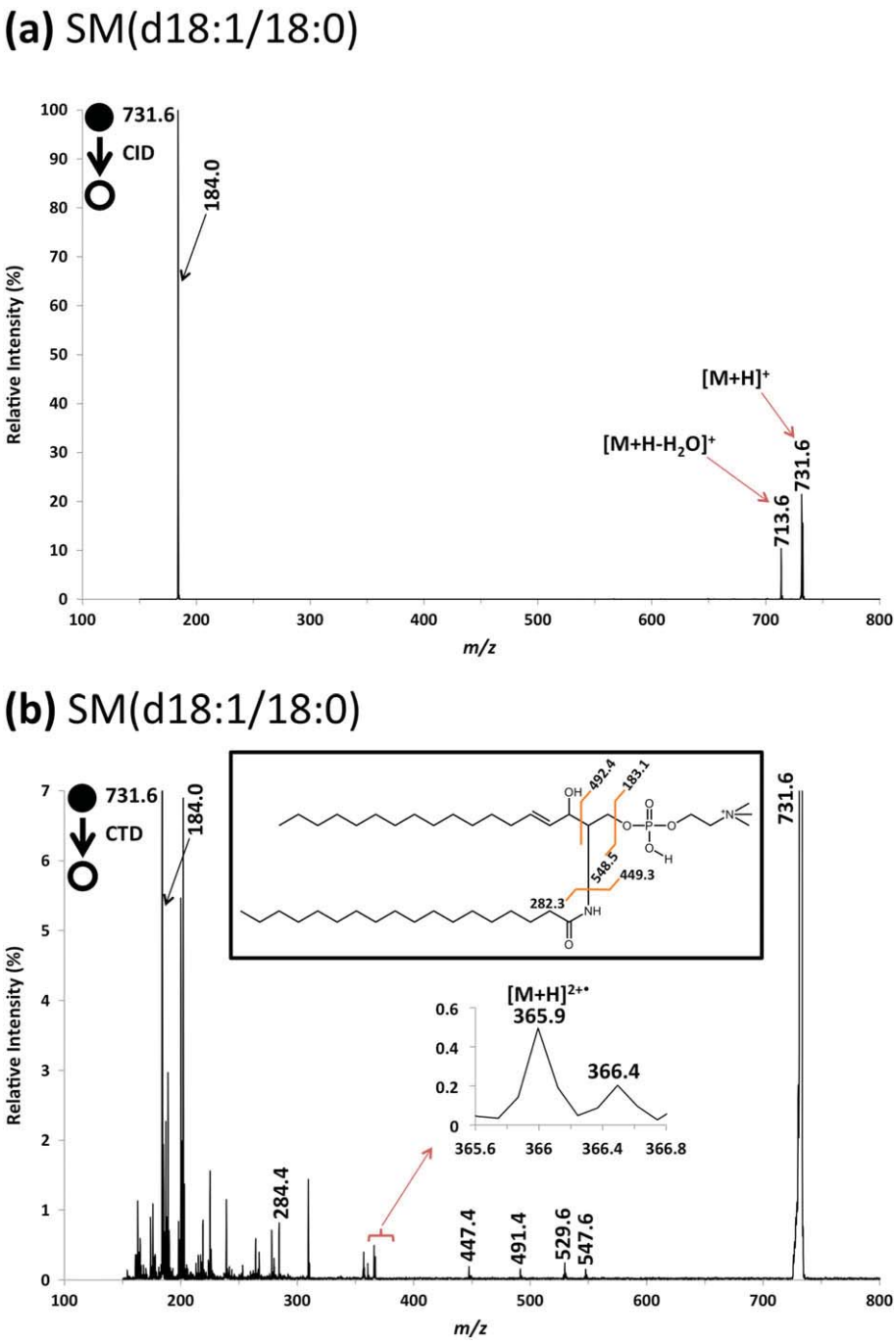


**Figure 7.** (a) Collision-induced dissociation (CID) spectrum of $[SM + H]^+$ (d181/180). (b) Charge transfer dissociation (CTD) spectrum of $[SM + H]^+$ (d181/180). [Colour figure can be viewed at wileyonlinelibrary.com]

Journal of MASS SPECTROMETRY

fragmentation upon the SM class using EIEIO/EID.[5] In addition to the lipid class information, their experiments were able to provide information regarding acyl group structure and the double bond (s) positioning for nearly 200 SM molecules.

Collision-induced dissociation and CTD spectra of $[DAPC + H]^+$ are shown in Fig. S5. Upon collisional activation, $[DAPC + H]^+$ mainly produces fragments corresponding to head group loss, sn-1/sn-2 fatty acid and alkyl ketene losses, which is quite similar to the pattern of CID of $[9E\text{-}/9Z\text{-}DOPC + H]^+$. CTD of DAPC produces the same cleavages but also produces 1+ and 2+ fragments in the vicinity of the four double bonds. The charge-increased product ion $[M + H]^{2+\bullet}$ at *m/z* 415.4 was generated, as was the case for all the examined phospholipids. The zoomed-in region from *m/z* 500 to 850 shows a relatively poor signal-to-noise ratio, which is inferior to that of MAD spectrum.[12] Consistent with MAD of DAPC, CTD of DAPC also produces quite limited cleavages, presumably because of the extra resonance stability afforded by the numerous double bonds.[12]

## Conclusions

Charge transfer dissociation MS (CTD-MS) has previously been shown as a promising alternative for structure interrogation of gas-phase peptide ions and complex carbohydrates.[17,27,43] Herein, we report CTD-MS on a different set of biomolecules—phospholipids—gives rise to helpful CID-like fragments, but also produces extensive dissociation within lipid acyl chains, which provides information that is not achievable through CID. The additional structural information includes the CC double bond positioning and possible the stereochemistry. Importantly, the diagnostic spacing of ion pairs is preserved across a range of lipids with varying acyl chain lengths and varying number of CC double bonds. If tested on a larger pool of lipids, CTD could be exploited to probe the structure of other classes of lipids or to the gas-phase chemistry of other biomolecules.

The quite poor signal-to-noise ratio and spectral complexity make CTD less appealing than OzID or other radical-induced methods, but improvements in efficiency and signal-to-noise could make CTD more appealing for lipid analyses in the future. For the lipids studied, CTD and MAD provide very similar fragmentation patterns and efficiencies, with neither technique having clear benefits over the other. In certain applications, it may be beneficial to have a beam of neutral reagent atoms that are unaffected by electric fields. In other applications, one may benefit from using a beam of helium cations to focus or steer the beam as desired.

### Acknowledgement

The authors acknowledge financial support from the National Institutes of Health (NIH) (1R01GM114494-01). The opinions, findings and conclusions or recommendations expressed in this publication are those of the author(s) and do not necessarily reflect the views of NIH.

## References

[1] J. Adams. Charge-remote fragmentations – analytical applications and fundamental-studies. *Mass Spectrom. Rev.* **1990**, *9*, 141.
[2] J. Adams, M. L. Gross. Charge-remote fragmentations of closed-shell ions – a thermolytic analogy. *J. Am. Chem. Soc.* **1989**, *111*, 435.
[3] K. A. Al-Saad, W. F. Siems, H. H. Hill, V. Zabrouskov, N. R. Knowles. Structural analysis of phosphatidylcholines by post-source decay matrix-assisted laser desorption/ionization time-of-flight mass spectrometry. *J. Am. Soc. Mass Spectrom.* **2003**, *14*, 373.
[4] Q. H. Ann, J. Adams. Collision-induced decomposition of sphingomyelins for structural elucidation. *Biol. Mass Spectrom.* **1993**, *22*, 285.
[5] T. Baba, J. L. Campbell, J. C. Y. Le Blanc, P. R. S. Baker. In-depth sphingomyelin characterization using electron impact excitation of ions from organics and mass spectrometry. *J. Lipid Res.* **2016**, *57*, 858.
[6] S. J. Blanksby, T. W. Mitchell. Advances in mass spectrometry for lipidomics. *Annu Rev Anal Chem (Palo Alto, Calif)* **2010**, *3*, 433.
[7] S. H. Brown, T. W. Mitchell, S. J. Blanksby. Analysis of unsaturated lipids by ozone-induced dissociation. *Biochim. Biophys. Acta* **2011**, *1811*, 807.
[8] B. A. Budnik, Y. O. Tsybin, P. Hakansson, R. A. Zubarev. Ionization energies of multiply protonated polypeptides obtained by tandem ionization in fourier transform mass spectrometers. *J. Mass Spectrom.* **2002**, *37*, 1141.
[9] J. L. Campbell, T. Baba. Near-complete structural characterization of phosphatidylcholines using electron impact excitation of ions from organics. *Anal. Chem.* **2015**, *87*, 5837.
[10] J. Castro-Perez, T. P. Roddy, N. M. Nibbering, V. Shah, D. G. McLaren, S. Previs, A. B. Attygalle, K. Herath, Z. Chen, S. P. Wang, L. Mitnaul, B. K. Hubbard, R. J. Vreeken, D. G. Johns, T. Hankemeier. Localization of fatty acyl and double bond positions in phosphatidylcholines using a dual stage cid fragmentation coupled with ion mobility mass spectrometry. *J. Am. Soc. Mass Spectrom.* **2011**, *22*, 1552.
[11] M. Claeys, L. Nizigiyimana, H. VandenHeuvel, P. J. Derrick. Mechanistic aspects of charge-remote fragmentation in saturated and mono-unsaturated fatty acid derivatives, evidence for homolytic cleavage. *Rapid Commun. Mass Spectrom.* **1996**, *10*, 770.
[12] R. E. Deimler, M. Sander, G. P. Jackson. Radical-induced fragmentation of phospholipid cations using metastable atom-activated dissociation mass spectrometry (MAD-MS). *Int. J. Mass Spectrom.* **2015**, *390*, 178.
[13] G. Dobson, W. W. Christie. Mass spectrometry of fatty acid derivatives. *Eur. J. Lipid Sci. Technol.* **2002**, *104*, 36.
[14] W. J. Griffiths, Y. Yang, J. A. Lindgren, J. Sjovall. Charge remote fragmentation of fatty acid anions in 400 ev collisions with xenon atoms. *Rapid Commun. Mass Spectrom.* **1996**, *10*, 21.
[15] L. Hejazi, D. Ebrahimi, M. Guilhaus, D. B. Hibbert. Discrimination among geometrical isomers of alpha-linolenic acid methyl ester using low energy electron ionization mass spectrometry. *J. Am. Soc. Mass Spectrom.* **2009**, *20*, 1272.
[16] Y. P. Ho, P. C. Huang. A novel structural analysis of glycerophosphocholines as tfa/k(+) adducts by electrospray ionization ion trap tandem mass spectrometry. *Rapid Commun. Mass Spectrom.* **2002**, *16*, 1582.
[17] W. D. Hoffmann, G. P. Jackson. Charge transfer dissociation (CTD) mass spectrometry of peptide cations using kiloelectronvolt helium cations. *J. Am. Soc. Mass Spectrom.* **2014**, *25*, 1939.
[18] F. F. Hsu, J. Turk. Structural determination of sphingomyelin by tandem mass spectrometry with electrospray ionization. *J. Am. Soc. Mass Spectrom.* **2000a**, *11*, 437.
[19] F. F. Hsu, J. Turk. Charge-remote and charge-driven fragmentation processes in diacyl glycerophosphoethanolamine upon low-energy collisional activation: a mechanistic proposal. *J. Am. Soc. Mass Spectrom.* **2000b**, *11*, 892.
[20] F. F. Hsu, J. Turk. Studies on phosphatidylglycerol with triple quadrupole tandem mass spectrometry with electrospray ionization: fragmentation processes and structural characterization. *J. Am. Soc. Mass Spectrom.* **2001**, *12*, 1036.
[21] F. F. Hsu, J. Turk. Electrospray ionization/tandem quadrupole mass spectrometric studies on phosphatidylcholines: the fragmentation processes. *J. Am. Soc. Mass Spectrom.* **2003**, *14*, 352.
[22] F. F. Hsu, J. Turk. Structural characterization of unsaturated glycerophospholipids by multiple-stage linear ion-trap mass spectrometry with electrospray ionization. *J. Am. Soc. Mass Spectrom.* **2008**, *19*, 1681.
[23] N. J. Jensen, K. B. Tomer, M. L. Gross. Gas-phase ion decompositions occurring remote to a charge site. *J. Am. Chem. Soc.* **1985**, *107*, 1863.
[24] J. W. Jones, C. J. Thompson, C. L. Carter, M. A. Kane. Electron-induced dissociation (EID) for structure characterization of glycerophosphatidylcholine: Determination of double-bond positions and localization of acyl chains. *J. Mass Spectrom.* **2015**, *50*, 1327.



  

[25] R. A. Klein. Mass spectrometry of the phosphatidylcholines: dipalmitoyl, dioleoyl, and stearoyl-oleoyl glycerylphosphorylcholines. *J. Lipid Res.* **1971a**, *12*, 123.
[26] R. A. Klein. Mass spectrometry of the phosphatidylcholines: fragmentation processes for dioleoyl and stearoyl-oleoyl glycerylphosphorylcholine. *J. Lipid Res.* **1971**, *12*, 628.
[27] P. Li, G. P. Jackson. Charge transfer dissociation (CTD) mass spectrometry of peptide cations: Study of charge state effects and side-chain losses. *J. Am. Soc. Mass Spectrom.* **2017**, https://doi.org/10.1007/s13361-016-1574-y.
[28] P. Li, W. D. Hoffmann, G. P. Jackson. Multistage mass spectrometry of phospholipids using collision-induced dissociation (CID) and metastable atom-activated dissociation (MAD). *Int. J. Mass Spectrom.* **2016**.
[29] X. Liang, J. Liu, Y. LeBlanc, T. Covey, A. C. Ptak, J. T. Brenna, S. A. McLuckey. Electron transfer dissociation of doubly sodiated glycerophosphocholine lipids. *J. Am. Soc. Mass Spectrom.* **2007**, *18*, 1783.
[30] X. Ma, Y. Xia. Pinpointing double bonds in lipids by paterno-buchi reactions and mass spectrometry. *Angew. Chem. Int. Ed. Engl.* **2014**, *53*, 2592.
[31] A. T. Maccarone, J. Duldig, T. W. Mitchell, S. J. Blanksby, E. Duchoslav, J. L. Campbell. Characterization of acyl chain position in unsaturated phosphatidylcholines using differential mobility-mass spectrometry. *J. Lipid Res.* **2014**, *55*, 1668.
[32] J. A. Madsen, T. W. Cullen, M. S. Trent, J. S. Brodbelt. IR and UV photodissociation as analytical tools for characterizing lipid a structures. *Anal. Chem.* **2011**, *83*, 5107.
[33] R. C. Murphy, K. A. Harrison. Fast atom bombardment mass spectrometry of phospholipids. *Mass Spectrom. Rev.* **1994**, *13*, 57.
[34] J. A. Op den Kamp. Lipid asymmetry in membranes. *Annu. Rev. Biochem.* **1979**, *48*, 47.
[35] H. T. Pham, T. Ly, A. J. Trevitt, T. W. Mitchell, S. J. Blanksby. Differentiation of complex lipid isomers by radical-directed dissociation mass spectrometry. *Anal. Chem.* **2012**, *84*, 7525.
[36] H. T. Pham, A. T. Maccarone, J. L. Campbell, T. W. Mitchell, S. J. Blanksby. Ozone-induced dissociation of conjugated lipids reveals significant reaction rate enhancements and characteristic odd-electron product ions. *J. Am. Soc. Mass Spectrom.* **2013**, *24*, 286.
[37] H. T. Pham, A. J. Trevitt, T. W. Mitchell, S. J. Blanksby. Rapid differentiation of isomeric lipids by photodissociation mass spectrometry of fatty acid derivatives. *Rapid Commun. Mass Spectrom.* **2013**, *27*, 805.
[38] A. Pluckthun, E. A. Dennis. Acyl and phosphoryl migration in lysophospholipids – importance in phospholipid-synthesis and phospholipase specificity. *Biochemistry-Us* **1982**, *21*, 1743.
[39] B. L. Poad, H. T. Pham, M. C. Thomas, J. R. Nealon, J. L. Campbell, T. W. Mitchell, S. J. Blanksby. Ozone-induced dissociation on a modified tandem linear ion-trap: observations of different reactivity for isomeric lipids. *J. Am. Soc. Mass Spectrom.* **2010**, *21*, 1989.
[40] M. Pulfer, R. C. Murphy. Electrospray mass spectrometry of phospholipids. *Mass Spectrom. Rev.* **2003**, *22*, 332.
[41] S. Ramanadham, A. Bohrer, R. W. Gross, J. Turk. Mass spectrometric characterization of arachidonate-containing plasmalogens in human pancreatic islets and in rat islet beta-cells and subcellular membranes. *Biochemistry-Us* **1993**, *32*, 13499.
[42] S. Rojas-Betancourt, J. R. Stutzman, F. A. Londry, S. J. Blanksby, S. A. McLuckey. Gas-phase chemical separation of phosphatidylcholine and phosphatidylethanolamine cations via charge inversion ion/ion chemistry. *Anal. Chem.* **2015**, *87*, 11255.
[43] D. Ropartz, P. Li, M. Fanuel, A. Giuliani, H. Rogniaux, G. P. Jackson. Charge transfer dissociation of complex oligosaccharides: comparison with collision-induced dissociation and extreme ultraviolet dissociative photoionization. *J. Am. Soc. Mass Spectrom.* **2016**, *27*, 1614.
[44] P. E. Siska. Molecular-beam studies of penning ionization. *Rev. Mod. Phys.* **1993**, *65*, 337.
[45] J. R. Stutzman, S. J. Blanksby, S. A. McLuckey. Gas-phase transformation of phosphatidylcholine cations to structurally informative anions via ion/ion chemistry. *Anal. Chem.* **2013**, *85*, 3752.
[46] M. C. Thomas, T. W. Mitchell, S. J. Blanksby. Ozonolysis of phospholipid double bonds during electrospray ionization: a new tool for structure determination. *J. Am. Chem. Soc.* **2006**, *128*, 58.
[47] M. C. Thomas, T. W. Mitchell, D. G. Harman, J. M. Deeley, R. C. Murphy, S. J. Blanksby. Elucidation of double bond position in unsaturated lipids by ozone electrospray ionization mass spectrometry. *Anal. Chem.* **2007**, *79*, 5013.
[48] M. C. Thomas, T. W. Mitchell, D. G. Harman, J. M. Deeley, J. R. Nealon, S. J. Blanksby. Ozone-induced dissociation: elucidation of double bond position within mass-selected lipid ions. *Anal. Chem.* **2008**, *80*, 303.
[49] V. H. Wysocki, M. M. Ross. Charge-remote fragmentation of gas-phase ions – mechanistic and energetic considerations in the dissociation of long-chain functionalized alkanes and alkenes. *Int. J. Mass Spectrom. Ion Proces* **1991**, *104*, 179.
[50] H. J. Yoo, K. Hakansson. Determination of double bond location in fatty acids by manganese adduction and electron induced dissociation. *Anal. Chem.* **2010**, *82*, 6940.
[51] N. Zehethofer, T. Scior, B. Lindner. Elucidation of the fragmentation pathways of different phosphatidylin ositol phosphate species (PIPX) using IRMPD implemented on a FT-ICR MS. *Anal. Bioanal. Chem.* **2010**, *398*, 2843.

## Supporting information

Additional Supporting Information may be found online in the supporting information tab for this article.